



Title	Binary functionalization of H:Si(111) surfaces by alkyl monolayers with different linker atoms enhances monolayer stability and packing
Author(s)	Arefi, Hadi H.; Nolan, Michael; Fagas, Gíorgos
Publication date	2016-04-12
Original citation	Arefi, H. H., Nolan, M. and Fagas, G. (2016) 'Binary functionalization of H:Si(111) surfaces by alkyl monolayers with different linker atoms enhances monolayer stability and packing', <i>Physical Chemistry Chemical Physics</i> , 18(18), pp. 12952-12963. doi: 10.1039/c5cp07601c
Type of publication	Article (peer-reviewed)
Link to publisher's version	http://dx.doi.org/10.1039/c5cp07601c Access to the full text of the published version may require a subscription.
Rights	© the Owner Societies 2016. This is the Accepted Manuscript version of a published work that appeared in final form in <i>Physical Chemistry Chemical Physics</i> . To access the final published version of record, see http://pubs.rsc.org/-/content/articlehtml/2016/cp/c5cp07601c
Item downloaded from	http://hdl.handle.net/10468/4944

Downloaded on 2018-08-23T19:06:25Z

Binary Functionalization of H:Si(111) Surface by Alkyl Monolayers with Different Linker Atoms Enhances Monolayer Stability and Packing

Hadi H. Arefi^{1,2}, Michael Nolan², and Giorgos Fagas²

¹ Department of Chemistry, Graduate School of Science, Kyoto University, Kyoto 606-8502, Japan,

² Tyndall National Institute, Lee Maltings, University College, Cork, Ireland,

E-mail: georgios.fagas@tyndall.ie

Abstract

Alkyl monolayer modified Si forms a class of inorganic-organic hybrid materials with applications across many technologies such as thin-films, fuel/solar-cells and biosensors. Previous studies have shown that the linker atom, through which the monolayer binds to the Si substrate, and any tail group in the alkyl chain, can tune the monolayer stability and electronic properties. In this paper we study the H:Si(111) surface functionalized with *binary* SAMs: these are composed of alkyl chains that are linked to the surface by two different linker groups. Aiming to enhance SAM stability and increase coverage over singly functionalized Si, we examine with density functional theory simulations that incorporate vdW interactions, a range of linker groups which we denote as $-X-(\text{alkyl})$ with $X = \text{CH}_2$,

O(H), S(H) or NH₂) (alkyl = C₆ and C₁₂ chains). We show how the stability of the SAM can be enhanced by adsorbing alkyl chains with two different linkers, e.g. Si-[C,NH]-alkyl, through which the adsorption energy is increased compared to functionalization with the individual -X-alkyl chains. Our results show that it is possible to improve stability and optimum coverage of alkyl functionalized SAMs linked through a direct Si-C bond by incorporating alkyl chains linked to Si through a different linker group, while preserving the interface electronic structure that determines key electronic properties. This is important since any enhancement in stability and coverage to give more densely packed monolayers will result in fewer defects. We also show that the work function can be tuned within the interval of 3.65 - 4.94 eV (4.55 eV for bare H:Si(111)).

1. Introduction

Systematic control of the surface properties and characteristics of semiconductors through well-defined surface modifications is an important challenge that is widely connected to different technological areas ranging from surface protection to high-technology topics such as medical implants or fabrication of biochips. Surface functionalization of silicon via chemisorption of self-assembled monolayers (SAMs)^{1, 2, 3} is a highly versatile approach, that is able to induce new chemical functionalities or properties into the surface or interface. Typically, a SAM consists of three major parts; the linker group, responsible for anchoring the SAM to the substrate, the tail group that is exposed and can be further functionalized and a spacer which separates the head and tail units and is usually an alkyl chain. In the usual SAM structure, the properties of the functionalized surface are primarily determined by the nature of the tail group.^{4, 5, 6} However, the linker that anchors the SAM to the surface is highly important as it determines the stability and coverage of the SAM on the surface.^{7, 8, 9, 10}

While single-component SAM functionalization is capable of tuning certain properties such as work function (WF)¹¹ or wettability⁴, applying a mixed monolayer, with two different components, has the potential to allow a range of surface properties to be tuned simply by adjusting in a rational manner the composition of the mixed monolayer.

In ref ⁴, it was shown that, for example, the wetting characteristics of gold surfaces can be tuned by mixed monolayers which contain both hydrophobic and hydrophilic components. In another work, the use of different ratios of two types of SAMs, namely n-alkanephosphonic and fluorinated phosphonic acid, which decrease and increase the WF, respectively, can tune the WF of indium-tin-oxide (ITO) over in the range of 5 - 5.75 eV (the WF of bare ITO is ~ 5.65 eV).¹² Chen et al showed that wetting and WF can be modified at the same time through mixed functionalization of fluorinated alkanethiol and a carboxyl-terminated alkanethiol on a silver substrate.¹³ Their investigation revealed that while changing the composition ratio can yield a WF in the range of 4.3 - 5.3 eV, adjusting the wettability depends on the chain lengths of the individual components. Xu et al.¹⁴ studied how charge injection can be regulated in an organic-field-effect-transistor (OFETs) structure using mixed SAMs of 1-decanethio (1DT) and perfluorodecanethiol (PFDT) to achieve a WF range of 4.4 - 5.6 eV.

Many binary monolayers such as aryl / alkyl¹¹ alkyl / alkyl¹⁵, fluoroalkyl / alkyl¹⁶, ester / alkyl¹⁷, haloalkyl / alkyl¹⁷, phthalimidoalkyl / alkyl¹⁸ and diphenylphosphino / alkyl¹¹ have been successfully fabricated on various types of silicon and silicon-dioxide substrates using organosilane mixtures. Contact angle measurement, X-ray photoelectron spectroscopy (XPS), atomic force microscopy (AFM) and ellipsometric thickness measurements have been used to characterise the fabricated SAMs^{19, 20} with an emphasis on composition and phase separation of the SAMs.^{5, 6} Mixtures of SAMs were presumed to create macroscopic islands, however later studies showed phase separation up to nanoscale level, for various binary n-Alkanethiols with long and short chains.^{21, 22} The distribution of each component in a mixed SAM is

determined by the type of functional group (linker and/or tail group), chain length and the fabrication process.^{23, 24} The study of combinations of short and long alkyl chain functionalization suggested the stability order to be long-long > short-short > long-short⁶ which clearly demonstrates the key role of mixed functionalization in determining the stability of the SAMs on metals. In one interesting application Frederix et al²⁵ studied a biosensor interface consisting of mixed SAMs of thiols with carboxylic and hydroxyl or poly (ethylene glycol) on gold. Their analysis based on surface plasmon resonance measurements showed that these mixed SAMs improve the sensitivity, stability, and selectivity in comparison with those of commercially available affinity biosensor interfaces.

In terms of electronic structure tuning, binary monolayers of n-alkanethiol (HDT) and the fluorinated analogue (FDT), in which the tail group is modified, attached to a silver surface can tune the WF over a wide range of 4.1 - 5.8 eV (WF of bare silver is 4.67 eV), by varying the ratio of the components.²⁶ A similar study on gold, using deposited alkanethiol SAMs with two different terminal groups, namely carboxylic acid and amine, reported a linear relationship between the concentration of each SAM and the surface WF; the WF varies within the boundaries set by functionalization with the corresponding single components.²⁷

Mixed functionalization can afford electronic tunability on semiconductor substrates.^{20, 27, 28,}

²⁹ Tong et al²⁰ investigated binary mixed SAMs of 3-aminopropyltriethoxysilane (APS, $\text{NH}_2(\text{CH}_2)_3\text{Si}(\text{OCH}_2\text{CH}_3)_3$) and octadecyltrimethoxysilane (ODS, $\text{CH}_3(\text{CH}_2)_{17}\text{Si}(\text{OCH}_3)_3$) on a silicon oxide surface. Their study revealed a strong influence of binary functionalization: introduction of APS induced a conformational disordering in the ODS SAM, which modifies the stability and the electronic properties. An investigation of Au nanoparticles modified by SAMs with mixed carboxylic acid and amine tail groups was presented by Lin et al³⁰ in which the surface potential and the iso-electric point (IEP) of the nanoparticles can be

modified by the ratio of these functional groups; the range of IEPs lies between the extremes defined by the amine and carboxylic acid functional groups.

There are fewer studies of binary functionalized semiconductor surfaces. O'Leary et al³¹ studied mixed methyl / allyl terminated-monolayers fabricated in a two-step halogenation / alkylation reaction process on Si(111). Their results indicated that the favourable properties of the methyl terminated SAM, such as effective passivation and the electrical properties can be maintained³² and a significant number of functional terminal groups (allyl) can be incorporated to allow secondary functionalization. The authors also showed that mixed SAMs on H:Si(111) functionalized with methyl and thienyl groups allow secondary functionalization to produce high-quality surfaces for tethering small molecules to silicon photoelectrodes and minimising residual electronic traps.³³

Smith et al³⁴ prepared a SAM composed of a mixture of aliphatic-aromatic species and they highlighted the homogeneity of the surface, nanoscale phase separation and high tunability of the compositions in a mixed fabricated aromatic-aliphatic trichlorinated SAM.

Computational studies on the subject of binary functionalization are less prominent. Rissner et al³⁵ investigated biphenylthiolate SAMs with $-NH_2$ and $-CN$ tail groups, adsorbed on the Au(111) surface using density functional theory (DFT). Their work, along with other computational studies on single-type functionalization on gold^{36, 37, 38, 39, 40} concludes that there is a sizable difference between the electronic structures of binary SAMs compared to single-component functionalized surface which they attributed to electrostatic interaction between the sublattices of the mixed-SAM components. An analysis of band-alignments and WF variation through altering the ratio of the two SAMs showed a linear change in the WF and band alignment with respect to the ratio of each SAM. Kuo et al⁴¹ presented a combined DFT and experimental study of binary siloxane-anchored SAMs with various ratios of 3-aminopropyltrimethoxysilane (APTMS, amine tail group) and 3-

mercaptopropyltrimethoxysilane (MPTMS, thiol end group) to demonstrate tuning of the WF. They concluded that the WF of silicon modified with these binary SAMs showed a linear dependence on the SAM composition, to allow tuning between extremes of each single type functionalization, giving a WF change of up to ~1.6 eV.

Despite the fact that the anchoring chemistry plays a key role in the stability and packing density of SAMs, the effect of binary linkers, in particular different combinations of linkers and various alkyl chain lengths, is not well understood. Therefore, in this work we investigate the effect of binary functionalization with different linkers and alkyl chain lengths. Furthermore, we emphasize the stability and coverage enhancement by applying suitable combinations of the binary components. As described before for single SAM functionalization different structural characteristics are possible that depend on the nature of the linking atom. Our analysis of the optimum coverage with binary linkers also exhibits a strong dependence on the nature of the linkers. From this, we propose the possibility to gain finer control in the adjustment of the WF and, most importantly, an improvement in SAM stability and coverage density by using a mixture of functionalization with binary linkers.

In our previous works^{7, 42} we have studied the effect of functionalization on the H:Si(111) surface with different linkers between the surface and SAM structure, focusing on the electronic and structural properties. We showed that different surface terminations can induce a variety of effects.⁴³ Direct alkyl chain attachment to Si through Si-[N, O, S] linkers rather than usual Si-C bond,^{44, 45, 46} can be used to control the stability and packing of a SAM on Si and WF tuning of the Si-SAM system.

A significant consequence of enhanced stability and higher packing density of SAMs on Si is a higher degree of ordering in the SAMs and consequently fewer defects. This will therefore improve the efficiency of the solid-molecule systems by eliminating the negative impact of structural defects. Binary functionalization may also allow for finer tuning of the WF.

Finally, binary functionalization can prepare a platform for secondary functionalization which is important in terms of fabricating those structures with desired functionalities. Figure 1 shows a schematic view of this concept.

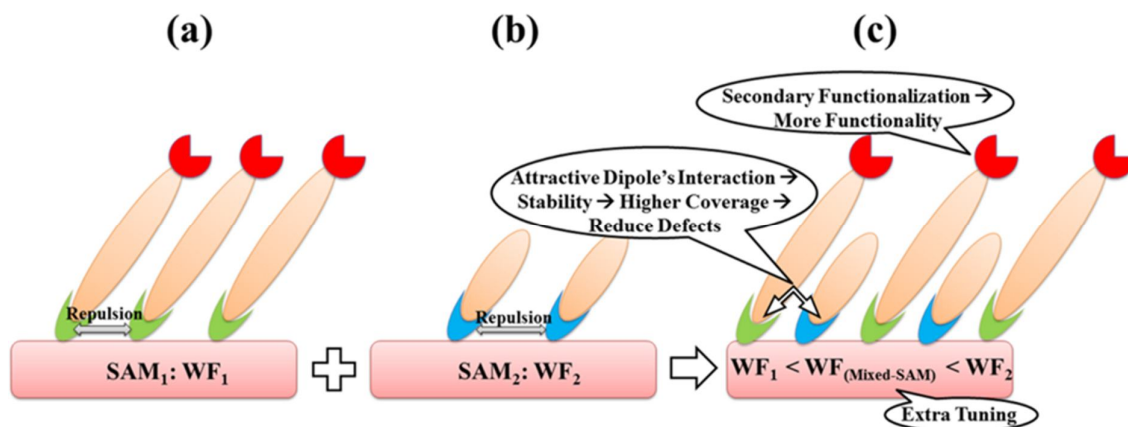


Figure 1. Conceptual demonstration of binary functionalization and its potential abilities: Single functionalization of each component has an absolute value of the surface WF with an optimum SAM coverage. See (a) and (b). With the careful choice of components, a mixed monolayer (c) may accommodate a higher coverage of SAMs as a result of attractive dipole interaction between each individual linker and as a result, stability enhancement of the final SAMs. Higher coverage is favourable since it helps reducing the defects by saturation of the adsorption sites and delivers a uniform space charge layer at the interface. In addition, binary functionalization makes it possible to tune the WF within the interval of the WF of single functionalization and controlling the coverage of each SAM can further increase the tuning. Keeping the option of secondary functionalization via tail groups open, while not studied in this work, is also another advantage of the mixed monolayers.

2. Methodology and Model Building

2.1 Computational Method

We use Density Functional Theory (DFT) with inclusion of vdW interactions to model modified H:Si(111) and calculate the WF; this allows us to separate the various contributions

to the change in WF after surface modification.⁴⁷ The need for inclusion of vdW interactions has been shown in a diverse range of systems, e.g. in refs. 7, 48, 49. We study the Si(111) surface because there are now well established experimental approaches to prepare clean Si(111) in well-defined structures, making comparisons to experiment possible. Unlike other Si surfaces, such as (100), the (111) surface does not undergo the reconstructions that can make it difficult to identify modifications of the electronic structure due to modification with alkyl chains or the reconstructions. Finally, given that we ultimately want to study modified Si nanowires, the high mobility (110) oriented nanowires (typically with hexagonal cross-sections) have 4 out of 6 (111)-oriented facets, so that the planar (111) surface can be used as a model of the dominant facet in Si nanowires. Given our general picture of the surface-alkyl interaction, it is most likely reasonable that other Si surfaces will show the same overall behaviour as the (111) surface.

DFT produces trends in the adsorbate-modified substrate WF in qualitative agreement with experiment.^{7, 43} We perform periodic supercell calculations using a plane wave basis set within the PWSCF code of the QUANTUM-ESPRESSO distribution,⁵⁰ with the PBE gradient corrected functional.⁵¹ The electron-ion interaction is described by ultrasoft pseudopotentials (USPPs) with the following number of valence electrons for each element: Si:4, C:4, N:5, O:6, S:6 and a one electron potential for hydrogen. The kinetic-energy cutoff for the plane wave basis was 35 Ry for the wave function and 400 Ry for the charge density. Starting from bulk lattice constant (5.43 Å), we built a six layer slab of silicon (111), while dangling bonds are saturated with hydrogen on both sides. Each surface is separated by nine equivalent vacuum layers. Different expansions of the hydrogenated unreconstructed (1×1) surface were created to give supercells that allow us to simulate target coverages.

Full ionic relaxation with the bottom hydrogens fixed was performed until the forces on all atoms were less than 0.01 eV/Å. The Brillouin-zone was sampled using a (8×8×1)

Monkhorst-Pack k -point sampling mesh with zero offset for the initial cell. For created supercells, an appropriate fraction of K -grid has been included based on the number of repetitions in each direction. The fixed occupation technique was employed using ten additional bands to ensure convergence of the electronic states. A dipole correction⁵² as well as the semi-empirical dispersion term (DFT-D2)^{53, 54} including vdW interactions,^{55, 56} was used as in previous work, where we showed that including the vdW interaction is required to describe even qualitatively the adsorption properties of these structures.⁷

The key quantities we investigate are the **Adsorption Energy** and the **Work Function** we describe the methodology here. The adsorption energy of a single type of alkyl chain is computed as follows⁷

$$E^{\text{ads}} = [E(\text{H:Si}(111)\text{-}[(\text{X}+\text{Y})\text{-Alkyl}]) + nE(\text{H}_2)] - [E(\text{X-Alkyl} + \text{Y-Alkyl}) + E(\text{H:Si}(111))], \quad (1)$$

Where $E(\text{H:Si}(111)\text{-}[(\text{X}+\text{Y})\text{-Alkyl}])$ is the total energy of alkyl chains adsorbed through linkers X and Y at the Si (111) surface, $E(\text{X-Alkyl} + \text{Y-Alkyl})$ denotes the total energy of the free-standing alkyl chains, with terminating groups HX- and HY-, in the gas phase (same supercell and technical parameters, no Si(111) surface, H is added to passivate the linker and relaxed to find the optimum geometry), $nE(\text{H}_2)$ is the total energy of n H_2 molecules, in which one H comes from the molecule and one H from the Si surface, and n depends on the surface coverage. Finally, $E(\text{H:Si}(111))$ is the total energy of the bare hydrogenated Si(111) surface. In this form of the adsorption energy, the modification for adsorption of a single type of X-Alkyl molecule is obvious.

Eq. (1) includes the inter-chain interactions of the surface modifiers in the reference energy of the gas phase molecules, in particular the vdW interactions between the Alkyl chains,

which are accounted for on both sides of Eq. (1)^{7,48,49}. If one were to compute the reference energy of the molecules individually and add them together, this gives a more stable adsorption energy as there are no vdW chain-chain interactions present in the calculation of the reference energy of the molecules. However, the qualitative trends in stability and hence our discussion are unaffected when using this approach. We prefer to use Eq. (1) as it accounts for the molecule chain-chain interactions in the gas phase.

The Work Function is computed^{42,43} by taking the relaxed atomic structure of the modified Si(111) surface and performing a standard calculation of the average electrostatic potential along the surface normal vector and finding the energy at which the potential is flat. This is the vacuum level, denoted E_{vac} . Extracting the Fermi energy, E^{F} , from a single point energy calculation at the relaxed atomic structure, the Work Function (WF, in eV) is defined as: $\text{WF} = E_{\text{vac}} - E^{\text{F}}$.

2.2 Si-SAM Models

With this background, we investigate binary functionalization of the silicon (111) surface with alkyl monolayers with different anchoring chemistry ($X = \text{C}, \text{N}, \text{O}, \text{S}$ linkers) to examine if they offer further flexibility for tuning stability, packing and the WF. To this end, first we recall from our previous studies^{7, 42} that (1) alkyl SAMs adsorbed through the oxygen linker are the most stable (irrespective of coverage), followed by N, S and C and (2) the nitrogen linker induces the largest shift in the WF of bare H:Si(111) among all our considered linking atoms. This is followed by oxygen, carbon and finally sulfur.

Thus, as the first step we fix the total coverage to 50% and study stability resulting from mixed functionalization of H:Si(111) surface with two from NH_2 , OH and SH terminations, each at 25% coverage, with no alkyl chain. We further study two different alkyl chain

lengths, namely hexane and dodecane, with these linkers. For coverage studies, binary SAMs of H:Si–X–hexane will be investigated.

In terms of terminology, almost all previous studies use the term “binary” to refer to a mixture of SAM with two different tail groups which implies tuning of the surface properties based on the choice of the components and the ratio of the mixture. However, in the present study the word “binary” will refer to SAMs with two different anchoring chemistries (that is the linkers) which will have different Linker–Si interactions and SAM structures that will modify the SAM stability, packing and electronic properties.

We have shown that functionalization of Si(111) with linkers other than carbon shows enhanced stability compared to Si–C bonding⁷ and a problem with direct alkyl-silicon attachment is that surface coverages larger than 50% cannot be accommodated. This has been shown from both theory^{7, 57} and experiment^{58, 59} and can result in defective SAMs which may limit the use in practical applications. Based on our results for different linkers, binary functionalization may be useful in avoiding this issue. However, it is important to remember that alkyl functionalization through a direct Si–C bond is widely used and there are many established synthesis techniques to functionalize surfaces in this way. Therefore, instead of creating an alkyl-functionalized surface with an altogether different linking atom to obtain higher coverages, which may not be straightforward in terms of experimental preparation and does not always result in higher coverage⁴⁶, increasing the Si–SAM coverage by adding Si–X–alkyl (X = NH, O, S) could be a more convenient approach to enhance stability and coverage; the latter is important as a more densely-packed monolayer is closer to an ordered crystal and is more controllable in terms of characteristics.^{60, 61}

3. Results and discussion

3.1. Stability with binary functionalization at fixed coverage

A schematic of the supercells used to model the SAM-modified H:Si(111) surfaces at different coverages is shown in Figure 2. The total coverage was first fixed to 50%, in which two out of the four terminating hydrogen are removed to allow adsorption of the SAM and the (2×2) cell (red-dashed parallelogram) is applied.

Based on their strong interaction with the H:Si(111) surface⁷ and their potential for tuning the WF^{42, 43}, we focus on three linkers, namely SH, OH, NH₂ and study binary combinations of these species with an emphasis on stability (the O linker gives high stability) and then on WF tuning (the NH linker gives the largest WF change compared to H:Si(111)).

The adsorption energy and WF were calculated for: (i) each binary system, with two alkyl chain lengths, that is, hexane and dodecane, and (ii) binary termination with only the linker groups.⁴³

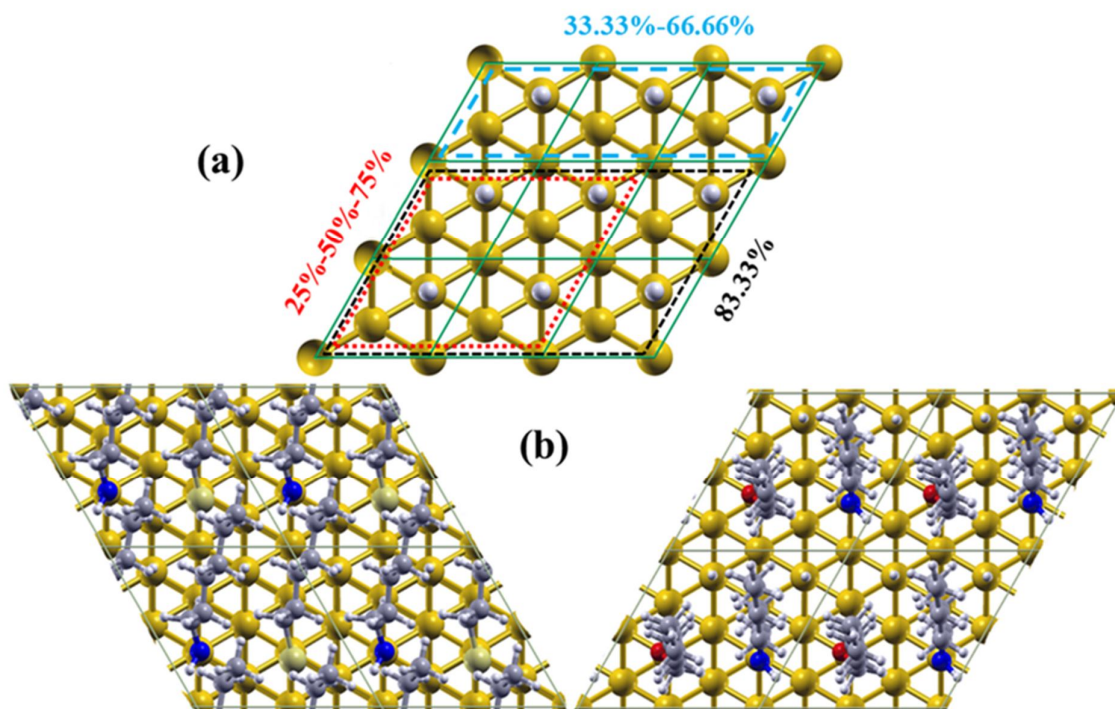


Figure 2. (a) Definition of the H:Si(111) supercell to allow the simulation of different SAM coverages: H:Si(111)-1 \times 3 with three adsorption sites was applied for total coverage of 66.6% (33.3% of each component). H:Si(111)-2 \times 2 cell with four adsorption sites was used to simulate total coverage of 50% (25% for each component) and 75% (25% plus 50% and vice versa). H:Si(111)-2 \times 3 cell with six adsorption sites implemented to simulate 83.33% (66.7% alkyl plus 16.7% another component) and full coverage (83.33% alkyl plus 16.7% other component) (b) Half covered binary SAMs with -NH-hexane / -S-hexane (left) and -NH-hexane / -O-hexane (right) simulated using a H:Si(111)-2 \times 2 cell after geometry optimization. Different coloured spheres stand for following atoms: Si = orange, H = white, C = grey, N = blue, O = red and S = yellow.

Adsorption energy: The adsorption energy is discussed for three cases: linker groups with no alkyl chain, a hexane chain and a dodecane chain and the computed adsorption energies for each case are shown in Table 1.

Table 1. Computed adsorption energies (in eV) for three classes of functionalization: termination with the linker (Si-XH) functionalization with hexane (Si-X-hexane) and functionalization with dodecane (Si-X-Dodecane). The surface coverage is fixed to 50% - 25% of each SAM in the case of binary functionalization.

Linker Groups (X)	Adsorption Energy (eV)		
	Si-XH	Si-X-hexane	Si-X-dodecane
<i>none</i> *	+0.15	-0.07	-0.17
-O	-0.72	-2.25	-2.13
-S	-0.58	-1.78	-1.80
-NH	-0.30	-1.20	-1.07
-(O + S)	-1.34	-1.88	-1.73
-(O + NH)	-0.80	-1.87	-1.73
-(S + NH)	-0.71	-1.97	-1.50

* i.e. no additional linker is added: the result is Si-H, Si-hexane and Si-dodecane.

For the case of termination groups without alkyl chain (Si-XH), the adsorption energy for the binary case lies lower than the adsorption energy of the individual linkers, thus giving enhanced stability. For example, from table 1, the adsorption energy of the OH + NH₂ binary functionalized surface is lower than that of the individual SAMs (OH: $E^{\text{ads}} = -0.72$ eV, NH₂: $E^{\text{ads}} = -0.30$ eV), with a computed adsorption energy of $E^{\text{ads}} = -0.8$ eV. There is an even bigger shift in the adsorption energy for the case of SH-OH ($E^{\text{ads}} = -1.34$ eV) functionalization compared to single OH ($E^{\text{ads}} = -0.72$ eV) or SH ($E^{\text{ads}} = -0.58$ eV) and similar differences are found in all cases.

Upon adding an alkyl chain to the linker, the (NH+S)-hexane monolayer shows similar trends to the linkers with no alkyl chains: for this particular binary system, the adsorption energy (-1.97 eV) is enhanced over S-hexane (-1.78 eV), while the adsorption energy for (NH+O)-hexane (-1.87 eV) is larger than NH-hexane (-1.20 eV). For an alkyl chain with 12 carbons, NH-dodecane is further stabilized in the binary system composed of the (NH+O)-dodecane SAM and the (NH+S)-dodecane SAM also shows enhanced stability compared to pure NH-dodecane functionalization.

We note that while binary combinations such as (S+O)-dodecane are less stable than functionalization with only the O or the S linker, this is simply related to the fact that for these longer chains the alkyl chain cannot take its preferred orientation within the binary functionalization scheme, arising from the presence of the second SAM. This therefore causes a reduction in the stability, as measured by the adsorption energies. However despite this, the computed adsorption energies for (S+O)-dodecane, S-dodecane and O-dodecane are -1.7 eV, -1.8 eV and -2.1 eV, respectively, which means the binary case is still very stable. For the shorter hexane chain this appears not to be as significant an issue and the stability of the binary structure is in between the strongest (O-dodecane) and weakest adsorbed (S-dodecane) SAM. In fact in ref⁷, we showed that different linkers, while having similar hexane chain structures, will show very different dodecane chain structures. The structure of the alkyl chain appears to be a key contributor to the stability in that if a SAM is not able to attain its preferred alkyl chain adsorption configuration, the stability is reduced, and in later sections, we will discuss its influence on SAM coverage and the WF change.

As discussed previously⁷, the adsorption energy can be driven by linker electronegativity and therefore charge transfer at the interface of the H:Si-[linker-(chain)]. Here we also include the van-der-Waals correction into the DFT-PBE calculations, necessary to describe Si-molecule interactions especially for long alkyl chains. In terms of electronegativity we know that the sequence is $\text{Si} < \text{S} < \text{N} < \text{O}$. However, when the H:Si(111) surface is terminated by -NH₂, -OH, -SH or mixture of the terminations, the single molecule electronegativity picture is not sufficient to assess the stability as the charge transfer could be completely distorted by surface effects, attached hydrogens for saturation of the dangling bonds and when an alkyl chain is attached through Si-X(H)-C bond (X = N, O, S). Structural properties, such as the structure of the alkyl chain play a more dominant role as the chain length is increased. The

nature of the linker can have a strong effect on the orientation of the chain and consequently the adsorption energy.

To examine this the optimized structure of the binary SAM, H:Si-[NH+(O/S)]-hexane / dodecane at half coverage is shown in Figure 3. The structures for functionalization with O-hexane / dodecane, S-hexane / dodecane and NH-hexane / dodecane at half coverage are also shown for comparison. The binary monolayers with the shorter hexane chain show smaller distortions from their most favourable configurations with a single linker. However the longer chain, dodecane, clearly shows more significant distortions compared to the adsorption structure with the single linker. This indicates that while the Si-linker interaction seems to be the main factor in determining the adsorption energy for short chain alkyls and therefore follows a trend whereby the adsorption energy is dominated by the more stable component, the significant chain-chain interactions and distortions for dodecane can modify this behaviour, thus giving different trends. The latter point is relevant as many experimental studies functionalize surfaces with long alkyl chains (usually for enhanced stability).

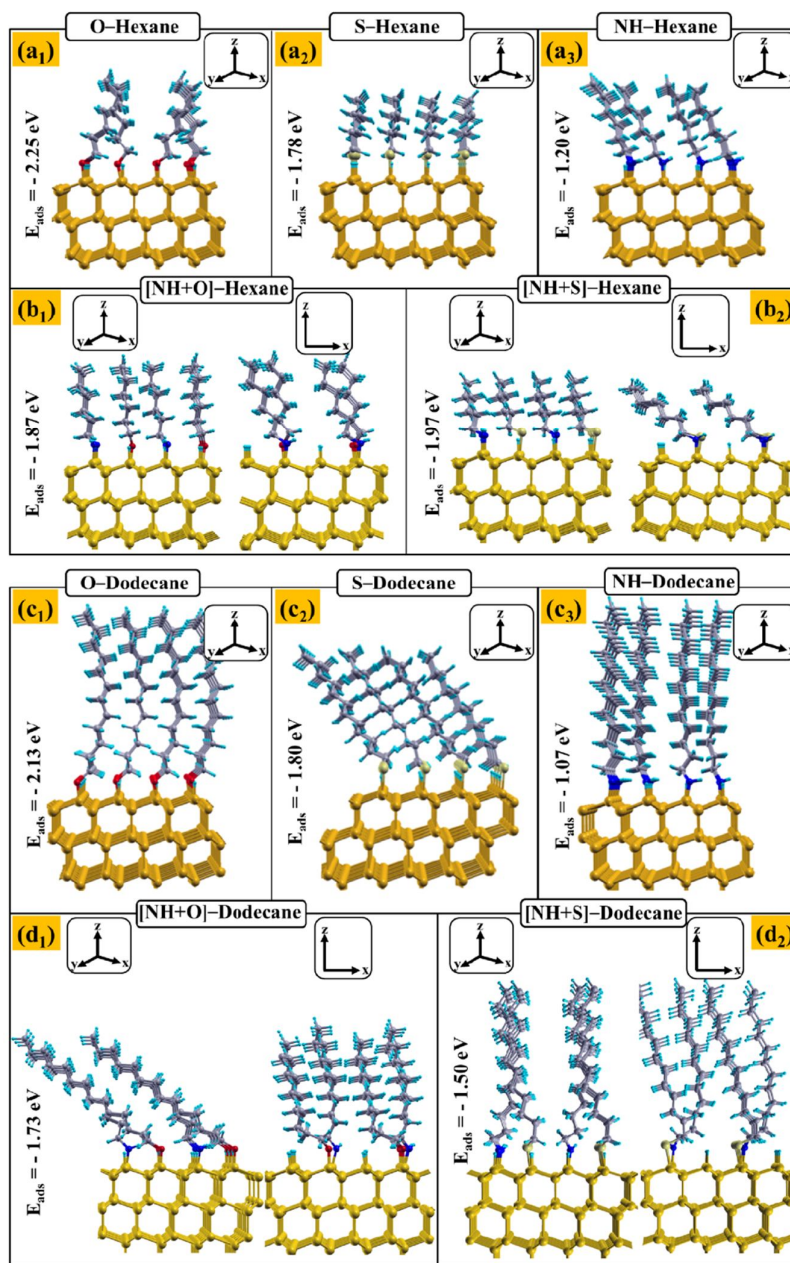


Figure 3. Atomic structures for single-type functionalization of H:Si(111) with O– (a₁), S– (a₂), NH–hexane (a₃) and the same for alkyl chain with 12 carbons (a_{4,5,6}). (b₁, b₂) Binary functionalized [NH+(O/S)]–hexane and (b₃, b₄) [NH+(O/S)]–dodecane for 50% coverage presented at two different views along z. Coloured spheres stand for following atoms: Si = orange, H = cyan, C = grey, N = blue, O = red and S = yellow. Adsorption energies are also presented for comparison.

Work function behaviour: In figure 4 (a, b, c) we present the computed WF for single functionalization and binary functionalization. For the case of linker-terminated H:Si(111) the computed WFs of the binary functionalized H:Si(111), with 25% coverage of each SAM, lie between the individual linker WF values at half coverage. The additive nature of the dipole moments has been shown for an individual linker-chain-terminal in previous studies and this directly influences the WF shift.^{39, 62} Therefore, if we consider that 50% coverage with linker X causes a shift of d_X in the WF compared to bare H:Si(111) surface and 50% coverage of linker Y gives a shift of d_Y , this additive picture suggest that mixed functionalization of (25%X + 25%Y) will give an approximate shift of $(d_X + d_Y)/2$ in the WF which qualitatively explains the average-like behaviour of the resulting WF from binary functionalization, compared with a single linker.

Figure 4 shows that for binary surface functionalization with the shorter $-X$ -hexane chains, the WF is the average of the value from single functionalization. However, this is not the case for the WF in the example of Si- X -dodecane functionalization; while the resulting WF lies within the two extremes of the individual WFs, the binary functionalized WF lies closer to the value for one linker than for the other. For the example of the Si-(O/NH)-dodecane system, the computed WF is 3.82 eV, which is closer to the WF of Si-O-dodecane (3.86 eV) than Si-NH-dodecane (3.52 eV).

To further understand the mechanism behind the behavior of the WF with binary functionalization from both the electronic and structural viewpoints, we consider the dipole analysis of two systems: first, the adsorbed $-XH$ and $-XC_6H_{13}$ terminations and monolayers (single and binary functionalization) on H:Si(111), with a fixed coverage of 50% and second the binary functionalization of H:Si(111) with $-O$ -dodecane and $-S$ -dodecane chains each at 25% coverage. We calculate the total, radical and effective dipole moments^{42, 43} of all modified H:Si(111) systems and these data are presented in Table 2.

Table 2. Total/Radical/Effective dipole moments (in Debye) of single and binary functionalized Si surface with XH / X-C₆H₁₃ (X = NH₂, OH and SH) at total 50% coverage. While total and radical dipole components were calculated in separate single-point energy calculations, effective dipole (bond dipole) is simply achieved by subtracting radical dipole from total dipole.

Termination	Total Dipole	Radical Dipole	Effective Dipole
-NH ₂	0.88	2.28	-1.40
-OH	0.15	1.53	-1.38
-SH	-0.52	0.17	-0.69
-(NH ₂ +OH)	0.38	1.61	-1.23
-(NH ₂ +SH)	0.12	1.20	-1.08
-(OH+SH)	-0.24	1.04	-1.28
Monolayer	Total Dipole	Radical Dipole	Effective Dipole
-NH-hexane	1.22	3.13	-1.91
-O-hexane	1.00	-0.17	1.17
-S-hexane	0.33	0.83	-0.50
-(NH+O)-hexane	1.11	2.99	-1.88
-(NH+S)-hexane	0.65	1.65	-1.00
-(O+S)-hexane	0.84	2.08	-1.24

We focus initially on the simpler case of –XH terminations only. Upon examining Table 2, we see that the effective dipole moment of the binary –(NH₂+OH) termination is smaller than either of the singly terminated modifications. This small deviation indicates that there is a less repulsive interaction between the terminal groups in the case of binary functionalization. This is of course controlled by the radical dipole, electronegativity and covalent radius of each individual termination which needs to be considered at the same time to interpret the resulting effective dipole. For example, in this case, the electronegativity of the O is slightly bigger than N (3.44 vs. 3.04) while N has slightly larger covalent radii than O (0.66 vs. 0.7 Å) and –NH₂ terminal has a much bigger radical dipole than –OH terminal. The upshot is that the combined –(NH₂+OH) terminations are less repulsive than either of them separately. In the other two cases, due to the much larger covalent radius of S (1.4 Å) but smaller electronegativity (2.58) and radical dipole compared to other two terminations, the change in the effective dipole (and adsorption energy) is more amplified. Both –(NH₂+SH) and –(OH+SH) terminations have effective dipoles that lie between the values of the singly

functionalized counterparts, with that of the $-(\text{NH}_2+\text{SH})$ termination being almost same as the average of the singly functionalised system. The effective dipole for the binary $-(\text{OH}+\text{SH})$ system is closer to that of the $-\text{OH}$ linked system. This indicates a more effective modulation by the binary terminations in the case of the latter. We attribute this to a smaller covalent radius of O and larger electronegativity difference with a relatively larger radical dipole compared to S. In contrast sulfur has a large covalent radius and small radical dipole. This interpretation is also in agreement with the computed adsorption energies in Table 1 where the binary $-(\text{OH}+\text{SH})$ termination delivers a lower adsorption energy, giving enhanced stability.

Once we add the alkyl chains to binary terminations, the situation gets more complex as the charge transfer along the linker-C bond as well as the chain dipole moment are extra variables which can also influence the effective dipole moment at the interface. Structural effects in the chains can also play a role, in particular due to the fact that each linker can induce different structural effects to the attached alkyl chain (direction, bend, twist etc.) and consequently the chains of different linkers interact with each other as well.

To address the structural analysis, we start with the optimized structure of $\text{H}:\text{Si}(111)-\text{O}$ -dodecane at 50% monolayer coverage and replace half of the linkers with sulfur and relax the structure (this is denoted Structure 1). The same procedure was also applied to $\text{H}:\text{Si}(111)-\text{S}$ -dodecane at 50% coverage, where half the S linkers are replaced with oxygen and the structure is relaxed (denoted Structure 2). The relaxed structures for Structure 1 and Structure 2 are shown in Figure 5.

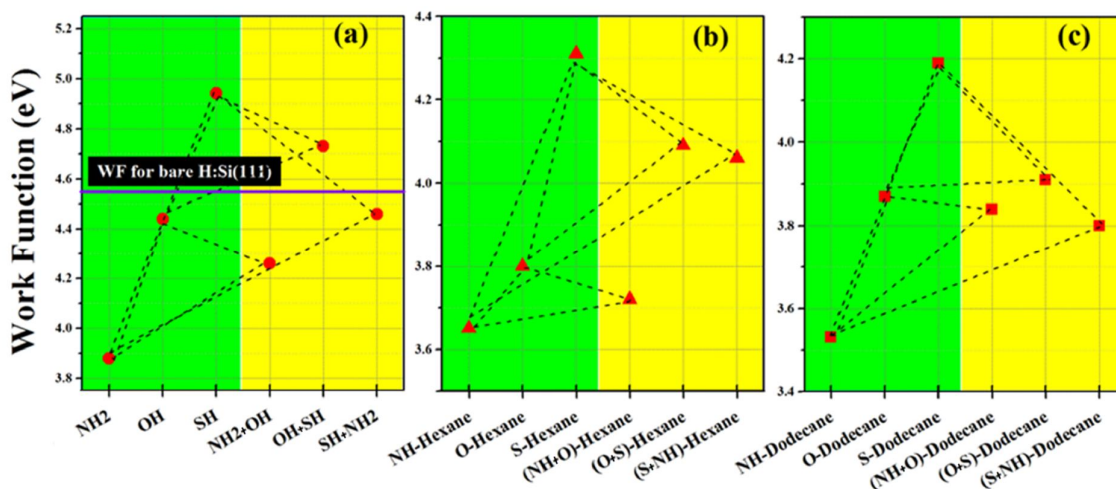


Figure 4. (a, b, c) WF for binary functionalized linker-(Chain)s at fixed (50%) coverage (yellow area); single functionalization (at 50% coverage) is also presented for comparison (green area). The horizontal purple line in (a) represent the WF of bare H:Si(111). Dashed triangles are connecting the WF values of binary functionalized structures to their single-type values at half coverage.

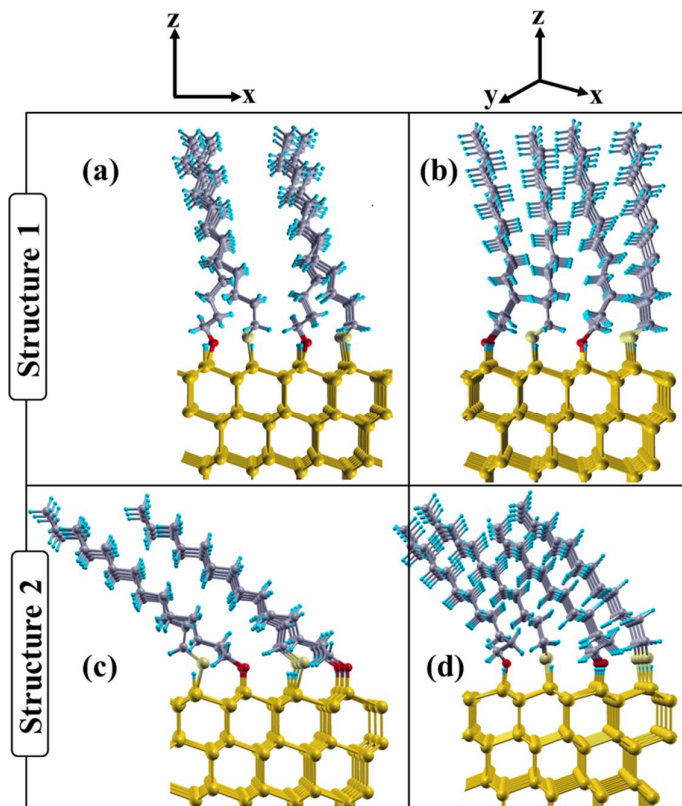


Figure 5. Structure 1: Optimized structure of binary functionalized silicon (111) with $-(O+S)$ -dodecane at half coverage (25% each) starting from H:Si(111)-O-dodecane structure showing two (a, b) cross-sections. Structure 2: Optimized structure of $-(O+S)$ -dodecane starting from relaxed H:Si(111)-S-dodecane at half coverage showing two (c, d) cross-sections.

It is interesting to observe that the relaxed structures for Structure 1 and Structure 2 are different, even though the computed adsorption energies are the same. As a consequence of the different relaxed structures, there is a 0.1 eV difference between the computed WFs with a WF of 3.87 eV for Structure 1 and 3.95 eV for structure 2. Recalling previous studies^{7, 42} we

know that monolayers with oxygen linker tend to stand upright and decrease the WF of H:Si(111) surface. In contrast, thiolated alkyls are less upright compared to SAMs with the oxygen linker and the decrease in the WF is smaller than for the oxygen linker. The structures in Figure 5 indicate that starting from an optimized monolayer with oxygen linker and adding S-dodecane will create a monolayer which is structurally more similar to the O-dodecane SAM and *vice versa*, so that the former shows a larger WF shift compared to the latter.

The WF is more sensitive to the chain orientation and length than the nature of the linker.⁴² Although the linker determines the SAM stability⁷ it does not in fact offer a wide range of WF tuning except for a shift that is constant for chains longer than six carbons.⁴² Therefore we suggest that in the case of binary monolayers, different chain orientations can lead to different shifts in the WF and this is governed by the linker group which forces the newly added alkyl chains to follow the initial monolayer direction. In the next section we also show that the orientation can further be controlled by the linker with higher coverage.

Based on these observations from DFT calculations for binary functionalization we suggest the following scheme. Functionalization of H:Si(111) with SAM₁ with orientation Θ_1 induces WF₁ and functionalization with SAM₂ with orientation Θ_2 , induces WF₂ (where WF₁ and WF₂ are different). In the binary functionalization scheme, if each monolayer keeps its initial orientation, which is the case with simple linker termination or hexane chains, then the final WF is (close to) the average value of WF₁ and WF₂. Now if SAM₂ has to follow the orientation of SAM₁ in the binary structure, and this is not the most stable orientation for SAM₂, then the resulting WF is going to lie within WF₁ and WF₂ but closer to WF₁ and *vice versa*. While the real situation will be more complex than this ideal case this does provides useful insights into the effect of binary functionalization on the WF of functionalized H:Si(111).

3.2. Binary functionalization for different coverage—Stability and Packing

In the previous section we investigated the effect of binary functionalization for combinations of –linker–(chains) with NH₂, OH and SH linkers and two lengths of alkyl chains –C₆ and –C₁₂ at a fixed surface coverage of 50% and compared the result with single functionalization at the same surface coverage. In this section we investigate if variation of the coverage in mixed-functionalization allows extra control to further tune stability and packing beyond the limited coverages available (maximum of 50%) for single linker-chain functionalization, with the aim to obtain increase coverage and hence stability of the SAMs on the H:Si(111) surface. For this purpose, we use an alkyl chain with a fixed chain length of six carbons and considered direct Si–C₆ bonds together with Si–NH–C₆ or Si–O–C₆ functionalization to examine if the inclusion of a second linker into the binary SAM can stabilize higher coverages, while maintaining the electronic properties resulting from alkyl functionalization that makes these structures attractive.

We start with 50% total coverage, that is 25% coverage of each linker, and then 66% total coverage (coverages are indicated in Figure 2), which is 33% coverage of each linker-chain. Then keeping the Si–C coverage at 33% we add 16.66% of the second linker, Si–(NH or O)–hexane, giving 50% total surface coverage. Next we consider Si–C at 50% and Si–(NH or O)–hexane at 16.66% (giving 66% total surface coverage) or 25% (giving 75% total surface coverage). Finally, we consider Si–C coverage at 66.66% or 83.33%, with the Si–(NH or O)–hexane coverage at 16.66%, giving 83% and 100% total surface coverage respectively. This gives all coverages from 50% to full coverage of the H:Si(111) surface. The results for WFs and adsorption energies are shown in Figure 6 and the optimized atomic structures for various ratio of Si–C bonding combined with either Si–NH or Si–O are presented in Figure 7. The

adsorption energies are calculated following the Eq. (1) described in the methodology section.

Considering first the computed adsorption energies, the addition of the second linker, be it O or NH, makes all SAM coverages more stable than with only Si–C linking. Particularly noteworthy is the significant enhancement of stability when the oxygen linker is introduced, which allows an increase in coverage of up to 75%; for only Si–C linked chains this coverage is not at all stable.⁷ It appears that higher coverages than 75%, are not stable but this is still a worthwhile enhancement in coverage. One could examine different proportions of the linkers at a total coverage of, say, 84% to see which, if any, mix of Si–C–alkyl and Si–O–alkyl would impart stability to such high coverages, although this may be ultimately determined by the ability to pack the alkyl chains in a favourable configuration. Finally, adding the oxygen linked alkyl chain always gives higher stability for a given coverage than adding nitrogen linked alkyl chains.

For these binary functionalized systems, the WF shift from that of the H:Si(111) surface with Si–C functionalization are quite small, being no larger than 0.2 eV at 83% surface coverage and even smaller at 75% and 66% coverages. The WF shift follows a general trend $[\text{Si–C} + \text{Si–N}] > \text{Si–C} > [\text{Si–C} + \text{Si–O}]$. Furthermore, the limited WF shift for SAMs composed of oxygen linked alkyl chains and Si–C–alkyl chains, compared to a SAM of only Si–C–alkyl, indicates that both the stability of the SAM and the total coverage on the H:Si(111) surface are enhanced, but the original electronic properties of the Si–alkyl SAMs are preserved.

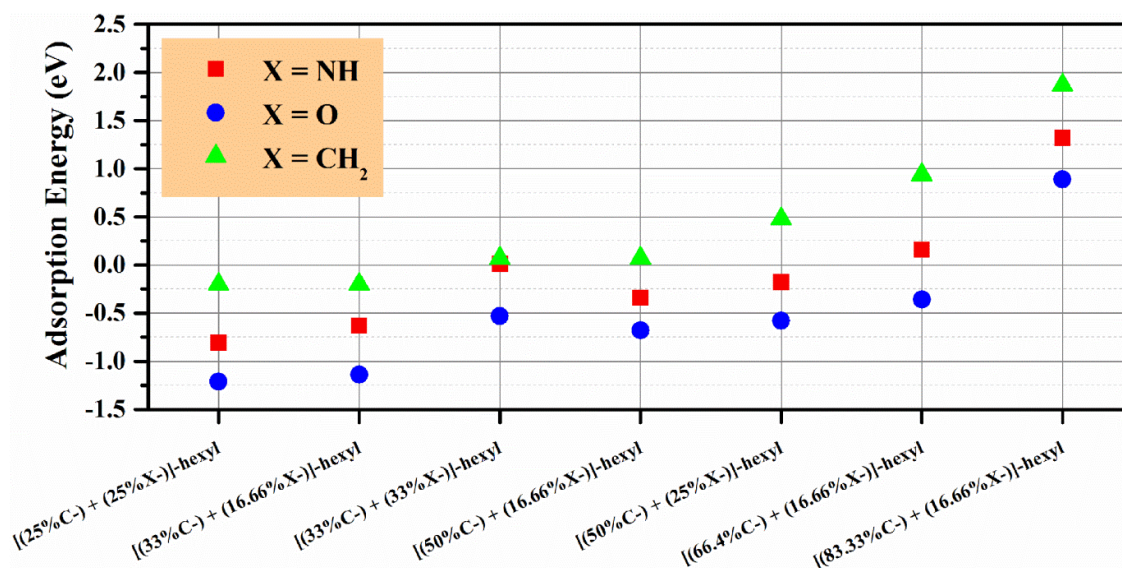


Figure 6. Adsorption energy for binary functionalized linker-(Chain)s for different ratio of (Si-C/Si-X)-hexane at half coverage [X = NH, O].

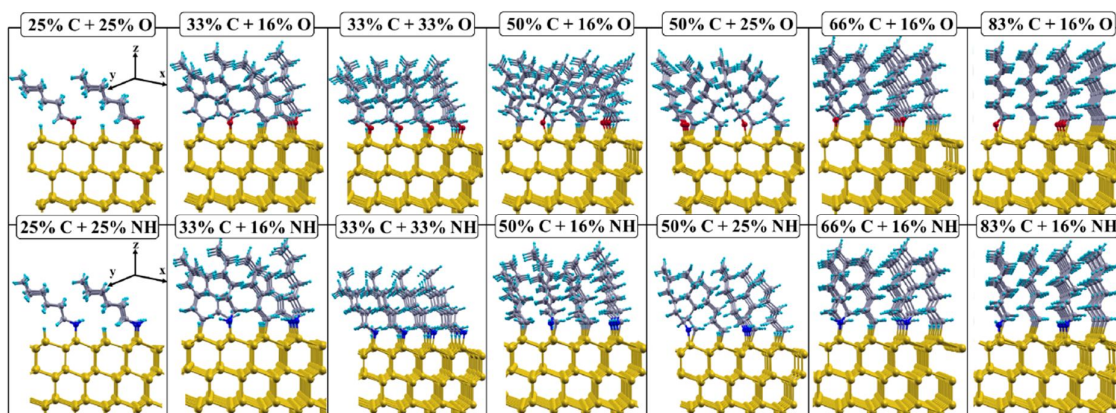


Figure 7. Relaxed atomic structures for binary SAMs of O-hexane + hexane (top panel) and NH-hexane + hexane (bottom panel) with different ratio of each component, specified inside the boxes, showing the view of the xy plane, along the z direction.

Thus, the properties of functionalized H:Si(111) that make it attractive for applications can still be comparable to the uniform Si-alkyl functionalized surface but adding the second linker-alkyl SAM helps in accommodating more alkyl chains than with direct Si-C bonding. To examine how the electronic structure is changed compared to the Si-C-alkyl

functionalized surface we undertake analysis of the integrated local density of state (ILDOS) analysis for [(25%/50%)–hexane + 25% –(NH/O)–hexane]. We averaged along the slab direction (z -direction) and plot the results for different structures (see Figure 8). The results in Figure 8 show that for a total surface coverage of 50% there are some differences between the binary and single type alkyl SAM interfacial ILDOS. However increasing the coverage up to 75%, gives an ILDOS that is similar for all SAMs, whether they be single functionalization or binary functionalization; for all structures, the ILDOS is unchanged in the silicon surface. The consequence of this is that the binary functionalization scheme can impart enhanced SAM stability, particularly at higher coverages, while leaving unchanged the electronic properties that are important for applications.

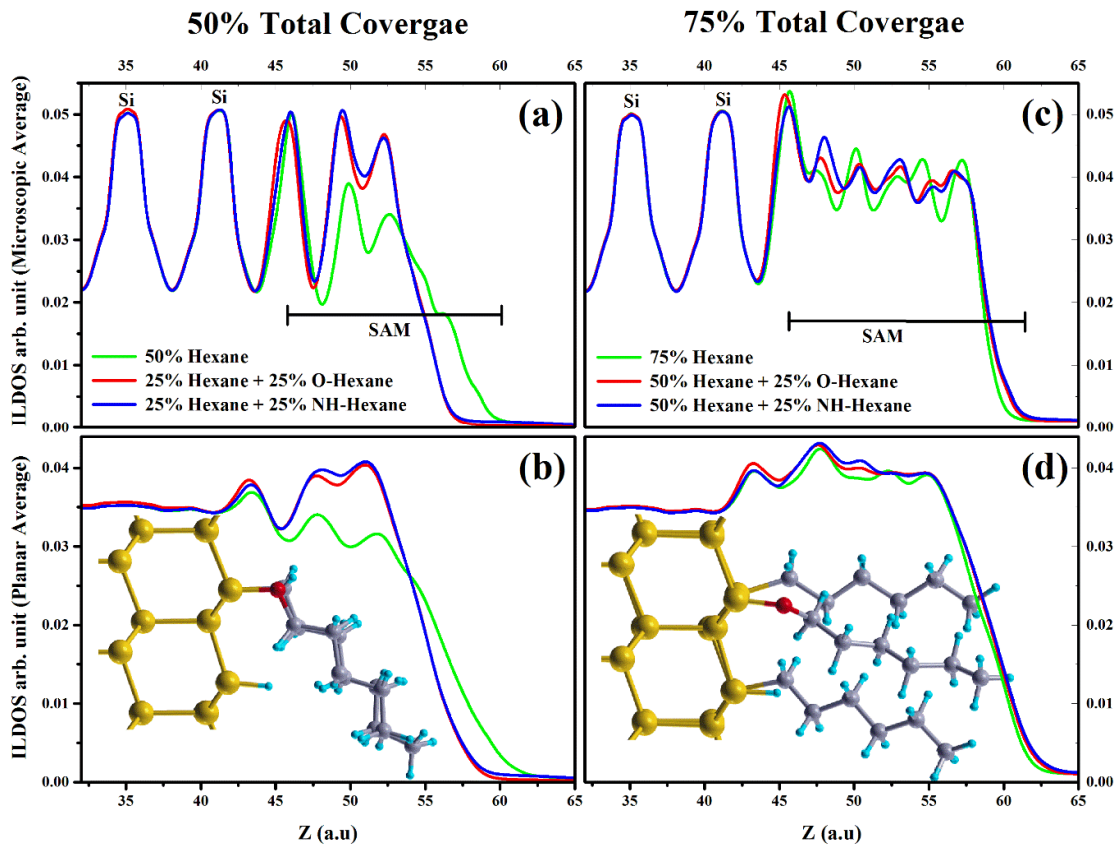


Figure 8. Planar and microscopic average of the integrated local density of states (ILDOS) for total coverage of 50% (a, b) and 75% (c, d) of H:Si(111)-hexane monolayers and binary combinations with -(NH/O)-hexane. The schematic of considered structure at each coverage is also presented in (b, d).

This can be further investigated by decomposing the lateral interactions between binary linking groups as follows: (i) van der Waals interaction as a result of correlated charge fluctuations. However this is less significant for covalently attached monolayers. (ii) Dipole interactions either due to permanent (radical) dipoles and/or bond dipoles. Regarding the repulsion/attraction for parallel/antiparallel dipoles, obtaining the desired properties is highly dependent on the correct choice of the binary components. (iii) Overlapping orbitals of neighbouring components can have a significant share in lateral interactions depending on how dense the monolayer is packed. (iv) The substrate-mediated interaction has two origins: (a) charge reorganization at the interface (accumulation/depletion) as a result of strong covalent bonding between surface atoms and the adsorbate which can penetrate a few Å into the substrate. This creates an indirect interaction between neighbouring adsorbates that depends on the types of components, either repulsive or attractive. (b) The adsorbate's strong covalent bond with the substrate can induce strain at the surface. Therefore depending on the elastic properties of the substrate, a similar interaction to (a) can occur. The substrate mediated effect (indirect) is normally less strong than the direct dipole-dipole interaction.

4. Concluding Remarks

Building on our understanding of functionalization of H:Si(111) with alkyl chains attached to the surface through different linker atoms and bearing in mind how the linker can determine SAM coverage and the electronic and structural properties, we have studied H:Si(111) functionalized with binary SAMs, that is with two SAMs having different linking atoms.

Aiming for enhanced SAM stability, higher surface coverage and WF adjustment, we chose a range of terminations and linker-chains denoted as $-X-(\text{alkyl})$ with $X = \text{CH}_3, \text{NH}_2, \text{O}(\text{H}), \text{S}(\text{H})$ and investigated the stability and change in WF of different binary SAMs attached to the H:Si(111) surface.

We firstly fix the total surface coverage of SAMs to 50% and examine different linking atoms with alkyl chains of the same chain length (each at 25% coverage) and calculated adsorption energy and WF. Comparing with the results for the corresponding single type of functionalization for each component we demonstrated that the binary SAMs are generally more stable. We also find that the conformations of long alkyl chains are important in determining the stability. There is also the possibility to obtain some fine tuning of the WF tuning as the computed WF lies within the limits of the WF for the individual linkers

In the second part of this work, we studied hexane monolayers with direct Si-C bonds to H:Si(111) combined with either $-\text{NH}-\text{hexane}$ or $-\text{O}-\text{hexane}$, as a model of H:Si-C-alkyl mixed with a second linker. We have shown that this binary functionalization stabilises coverages larger than 50%. Very small WF changes are observed upon binary functionalization at higher coverages and examination of the electronic properties shows that the attractive features of Si-C linked SAMs are not affected by inclusion of the second type of SAM.

In summary:

- 1) Binary functionalization can enhance the SAM stability. Direct Si-C grafted SAMs are less stable compared to those with N, O or S linkers. Regardless of the ratio, binary functionalized alkyl monolayers with NH, O or S linkers are always more stable than single type alkyl functionalization with the same coverage.
- 2) Our results indicate that it is possible to go beyond the optimum coverage of pure alkyl functionalized SAMs (50%) by adding a suitable choice of linker.

- 3) Using binary functionalization with $-\text{[NH}_{2\text{)/O(H)/S(H)]-}$ [hexane / dodecane] as the second SAM, we showed that with enhanced coverage, there is only a small change in the WF compared to Si-C-alkyl. This is very important since dense packed monolayers have fewer defects and deliver higher efficiency in their broad range of applications.

5. Acknowledgment

We acknowledge support from the European Commission, through the 7th Framework Programme ICT FET-Proactive Projects: SiNAPS (contract no 257856) and ICT-Energy (contract no 611004). M.N. acknowledges the Science Foundation Ireland (SFI) Starting Investigator Research Grant Programme, project EMOIN grant number SFI 09/SIRG/I1620 and SFI US-Ireland R&D Partnership Program, project "SusChem" grant number SFI 14/US/E2915. H.A. also acknowledges partial support from the SFI project ALDesign grant number 09/IN.1/I2628. Computing resources were provided by SFI to the Tyndall National Institute and the Irish Centre for High End Computing. We thank Dr. Simon Elliott for critical review of an early version of the manuscript and fruitful discussions.

6. References

1. A. Ulman, *Chem. Rev.* 1996, 96, 1533-1554.
2. G. M. Whitesides, *Scientific American* 1995, (September), 146-149.
3. G. M. Whitesides and B. Grzybowski, *Science*, 2002, 295, 2418-21.
4. J. P. Folkers, P. E. Laibinis, G. M. Whitesides and J. Deutch, *J. Phys. Chem.* 1994, 98, 563-571.

5. C. D. Bain, E. B. Troughton, Y. T. Tao, J. Evall, G. M. Whitesides and R. G. Nuzzo, *Journal of the American Chemical Society* 1989, *111*, 321-335.
6. J. P. Folkers, P. E. Laibinis and G. M. Whitesides, *Langmuir* 1992, *8*, 1330-1341.
7. H. H. Arefi, M. Nolan and G. Fagas, *Langmuir* 2014, *30*, 13255-13265.
8. S. Gangarapu, S. P. Pujari, H. Alon, B. Rijksen, C. N. Sukenik and H. Zuilhof, *Langmuir* 2015, *31*, 8318-8327.
9. T. Toledano, R. Garrick, O. Sinai, T. Bendikov, A.-E. Haj-Yahia, K. Lerman, H. Alon, C. N. Sukenik, A. Vilan, L. Kronik and D. Cahen, *Journal of Electron Spectroscopy and Related Phenomena* 2015, *204A*, 149-158.
10. M. Carbone, *Computational and Theoretical Chemistry* 2015, *1073*, 106-115.
11. J.-F. Erard, L. Nagy and E. S. Kovats, *Colloids and Surfaces* 1984, *9*, 109-132.
12. S.-Y. Yu, D. C. Huang, Y.-L. Chen, K.-Y. Wu and Y.-T. Tao, *Langmuir* 2011, *28*, 424-430.
13. C.-Y. Chen, K.-Y. Wu, Y.-C. Chao, H.-W. Zan, H.-F. Meng and Y.-T. Tao, *Organic Electronics* 2011, *12*, 148-153.
14. Y. Xu, K.-J. Baeg, W.-T. Park, A. Cho, E.-Y. Choi and Y.-Y. Noh, *ACS Applied Materials & Interfaces* 2014, *6*, 14493-14499.
15. D. A. Offord, and J. H. Griffin, *Langmuir* 1993, *9*, 3015-3025.
16. J.-Y. Huang, K. J. Song, A. Lagoutchev, P. K. Yang and T. J. Chuang, *Langmuir* 1997, *13*, 58-64.
17. G. E. Fryxell, P. C. Rieke, L. L. Wood, M. H. Engelhard, R. E. Williford, G. L. Graff, A. A. Campbell, R. J. Wiacek, L. Lee and A. Halverson, *Langmuir* 1996, *12*, 5064-5075.
18. S. Heid, F. Effenberger, K. Bierbaum and M. Grunze, *Langmuir* 1996, *12*, 2118-2120.
19. M. Mansueto, S. Sauer, M. Butschies, M. Kaller, A. Baro, R. Woerner, N. H. Hansen, G. Tovar, J. Pflaum and S. Laschat, *Langmuir*, *28*, 8399-8407.

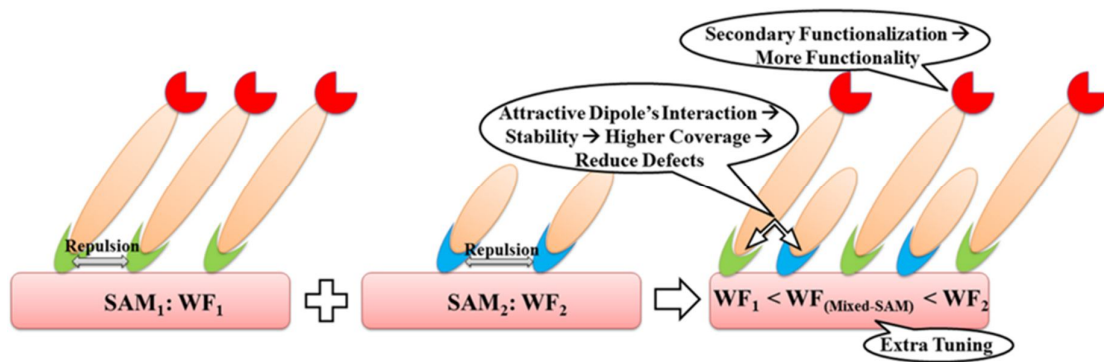
20. Y. Tong, E. Tyrode, M. Osawa, N. Yoshida, T. Watanabe, A. Nakajima and S. Ye, *Langmuir* 2011, 27, 5420-5426.
21. S.-i. Imabayashi, N. Gon, T. Sasaki, D. Hobara and T. Kakiuchi, *Langmuir* 1998, 14, 2348-2351.
22. F. Fan, C. Maldarelli and A. Couzis, *Langmuir* 2003, 19, 3254-3265.
23. F. Tielens, D. Costa, V. Humblot and C.-M. Pradier, *J. Phys. Chem. C* 2007, 112, 182-190.
24. B. Lüssem, L. Müller-Meskamp, S. Karthäuser, R. Waser, M. Homberger and U. Simon, *Langmuir* 2006, 22, 3021-3027.
25. F. Frederix, K. Bonroy, W. Laureyn, G. Reekmans, A. Campitelli, W. Dehaen and G. Maes, *Langmuir* 2003, 19, 4351-4357.
26. K.-Y. Wu, S.-Y. Yu, and Y.-T. Tao, *Langmuir* 2009, 25, 6232-6238.
27. S.-H. Lee, W.-C. Lin, C.-J. Chang, C.-C. Huang, C.-P. Liu, C.-H. Kuo, H.-Y. Chang, Y.-W. You, W.-L. Kao, G.-J. Yen, D.-Y. Kuo, Y.-T. Kuo, M.-H. Tsai and J.-J. Shyue, *Phys. Chem. Chem. Phys.* 2011, 13, 4335-4339.
28. C.-H. Kuo, H.-Y. Chang, C.-P. Liu, S.-H. Lee, Y.-W. You and J.-J. Shyue, *Phys. Chem. Chem. Phys.* 2011, 13, 3649-3653.
29. C.-H. Kuo, C.-P. Liu, S.-H. Lee, H.-Y. Chang, W.-C. Lin, Y.-W. You, H.-H. Liao and J.-J. Shyue, *Phys. Chem. Chem. Phys.* 2011, 13, 15122-15126.
30. Y.-C. Lin, B.-Y. Yu, W.-C. Lin, S.-H. Lee, C.-H. Kuo and J.-J. Shyue, *Journal of Colloid and Interface Science* 2009, 340, 126-130.
31. L. E. O'Leary, E. Johansson, B. S. Brunschwig and N. S. Lewis, *J. Phys. Chem. B* 2010, 114, 14298-14302.
32. K. T. Wong and N. S. Lewis, *Acc. Chem. Res.* 2014, 47, 3037-3044.

33. L. E. O'Leary, M. J. Rose, T. X. Ding, E. Johansson, B. S. Brunshwig and N. S. Lewis, *J. Am. Chem. Soc.* 2013, *135*, 10081-10090.
34. M. B. Smith, K. Efimenko, D. A. Fischer, S. E. Lappi, P. K. Kilpatrick and J. Genzer, *Langmuir* 2007, *23*, 673-683.
35. F. Rissner, D. A. Egger, L. Romaner, G. Heimel and E. Zojer, *ACS Nano* 2010, *4*, 6735-46.
36. G. Heimel, L. Romaner, E. Zojer and J. L. Bredas, *Nano Lett.* 2007, *7*, 932-940.
37. G. Heimel, L. Romaner, E. Zojer and J. L. Bredas, *Acc. Chem. Res.* 2008, *41*, 721-729.
38. A. Natan, L. Kronik, H. Haick and R. T. Tung, *Adv. Mater.* 2007, *19*, 4103-4117.
39. M. L. Sushko and A. L. Shluger, *Adv. Funct. Mater.* 2008, *18*, 2228-2236.
40. J.-G. Wang, E. Prodan, R. Car, and A. Selloni, *Phys. Rev. B* 2008, *77*, 245443/1-245443/8.
41. C. H. Kuo, C. P. Liu, S. H. Lee, H. Y. Chang, W. C. Lin, Y. W. You, H. Y. Liao and J. J. Shyue, *Phys. Chem. Chem. Phys.* 2011, *13*, 15122-15126.
42. H. H. Arefi, M. Nolan and G. Fagas, *J. Phys. Chem. C* 2015, *119*, 11588-11597.
43. H. H. Arefi and G. Fagas, *J. Phys. Chem. C* 2014, *118*, 14346-14354.
44. M. R. Linford and C. E. D. Chidsey, *J. Am. Chem. Soc.* 1993, *115*, 12631-12632.
45. J. M. Buriak, *Chem. Comm.* 1999, 1051-1060.
46. K. Uosaki, H. Fukumitsu, T. Masuda and D. Qu, *Phys. Chem. Chem. Phys.* 2014, *16*, 9960-9965.
47. L. Segev, A. Salomon, A. Natan, D. Cahen, L. Kronik, F. Amy, C. K. Chan and A. Kahn, *Phys. Rev. B* 2006, *74* (16), 165323/1-165323/6.
48. G. Li, I. Tamblyn, V. R. Cooper, H-J. Gao, and J. B. Neaton, *Phys. Rev. B* 2012, *85*, 121409/1 – 121409/4.

49. M. Yu, P. Doak, I. Tamblyn and J. B. Neaton, *J. Phys. Chem. Lett.* 2013, 4, 1701-1706.
50. P. Giannozzi, S. Baroni, N. Bonini, M. Calandra, R. Car, C. Cavazzoni, D. Ceresoli, G. L. Chiarotti, M. Cococcioni, I. Dabo, A. Dal Corso, S. de Gironcoli, S. Fabris, G. Fratesi, R. Gebauer, U. Gerstmann, C. Gougoussis, A. Kokalj, M. Lazzeri, L. Martin-Samos, N. Marzari, F. Mauri, R. Mazzarello, S. Paolini, A. Pasquarello, L. Paulatto, C. Sbraccia, S. Scandolo, G. Sclauzero, A. P. Seitsonen, A. Smogunov, P. Umari, R. M. Wentzcovitch, *J. Phys. Condens. Matter* 2009, 21, 395502/1-395502/19.
51. J. P. Perdew, K. Burke, M. Ernzerhof, *Phys. Rev. Lett.* 1996, 77, 3865-3868.
52. L. Bengtsson, *Phys. Rev. B* 1999, 59, 12301-12304.
53. S. Grimme, *J. Comput. Chem.* 2006, 27, 1787-1799.
54. V. Barone, M. Casarin, D. Forrer, M. Pavone, M. Sambri and A. Vittadini, *J. Comput. Chem.* 2009, 30, 934-939.
55. D. C. Langreth, B. I. Lundqvist, S. D. Chakarova-Kack, V. R. Cooper, M. Dion, P. Hyldgaard, A. Kelkkanen, J. Kleis, L. Kong, S. Li, P. G. Moses, E. Murray, A. Puzder, H. Rydberg, E. Schroder and T. A. Thonhauser, *J. Phys. Condens. Matter.* 2009, 21, 084203/1-084203/8.
56. K. Lee, E. D. Murray, L. Z. Kong, B. I. Lundqvist and D. C. Langreth, *Phys. Rev. B* 2010, 82, 081101/1-081101/4.
57. A. B. Sieval, B. van den Hout, H. Zuilhof and E. J. R. Sudhölter, *Langmuir* 2001, 17, 2172-2181.
58. D. J. Michalak, S. Rivillon, Y. J. Chabal, A. Estève and N. S. Lewis, *J. Phys. Chem. B* 2006, 110, 20426-20434.
59. X. Wallart, C. Henry de Villeneuve and P. Allongue, *J. Am. Chem. Soc.* 2005, 127, 7871-7878.

60. Y. Li, S. Calder, O. Yaffe, D. Cahen, H. Haick, L. Kronik and H. Zuilhof, *Langmuir* 2012, 28, 9920-9929.
61. J. L. Lou, H. W. Shiu, L. Y. Chang, C. P. Wu, Y. L. Soo and C. H. Chen, *Langmuir* 2011, 27, 3436-3441.
62. D. M. Alloway, M. Hofmann, D. L. Smith, N. E. Gruhn, A. L. Graham, R. Colorado, V. H. Wysocki, T. R. Lee, P. A. Lee and N. R. Armstrong, *J. Phys. Chem. B* 2003, 107, 11690-11699.

Table of Contents Graphic



Functionalization of H-terminated Si(111) with alkyl monolayers using two linker groups enhances monolayer stability and can tune the work function.